MICHIGAN STATE
UNIVERSITY

National Superconducting Cyclotron Laboratory

ANALYSIS OF THE INJECTION LINE FOR THE UNIVERSITY OF MARYLAND ELECTRON RING INCLUDING DISPERSION AND SPACE CHARGE

L.G. VOROBIEV and R.C. YORK

MSUCL-1122

JANUARY 1999

ANALYSIS OF THE INJECTION LINE FOR THE UNIVERSITY OF MARYLAND ELECTRON RING INCLUDING DISPERSION AND SPACE CHARGE

L.G.Vorobiev and **R.C.York**

National Superconducting Cyclotron Laboratory
Michigan State University
East Lansing, MI 48824

Abstract

An analysis of an injection line for the University of Maryland electron ring has been done where the matching requirements include six beam parameters – the envelopes (4 constraints) and the horizontal dispersion function (2 constraints). The physical model used to describe the high current beam dynamics includes space charge in the presence of dispersion. Two possible injection scenarios were evaluated. Within the limitation of the model, solutions compatible with the periodical dynamics in the ring were achieved for a dimensionless perveance (K) of 1.5 x 10^{-3} and a relative rms momentum spread (as) of 1.5 x 10^{-2}.

1. Introduction

The basic ring parameters assumed where those given in reference 1. Previous studies of the injection line[2] design were based on the standard rms envelope equations[3] that do not include dispersion. In the analysis following, the injection line parameters are obtained from a fitting algorithm based on a generalized set of rms envelope equations[4] that evolve all six parameters ($\sigma_{x,y}$, $\sigma'_{x,y}$ and D_x, D'_x) using a coupled-set of six equations.

2. Physical Model and Fitting Algorithm.

The rms envelope equations[3] have the form:

$$\sigma_x''+k_x(s)\sigma_x-\frac{K}{2(\sigma_x+\sigma_y)}-\frac{\varepsilon_x^2}{\sigma_x^3}=0 \qquad (1)$$

$$\sigma_y''+k_y(s)\sigma_y-\frac{K}{2(\sigma_x+\sigma_y)}-\frac{\varepsilon_y^{\,2}}{\sigma_y^{\,3}}=0 \tag{2}$$

Where $\sigma_{x,y}$ are the rms transverse beam sizes, K the generalized perveance, and $\varepsilon_{x,y}$ the rms transverse emittances. The dispersion function $D(s)$ in the absence of space charge is given by:

$$D''+k_x(s)D(z)=\frac{1}{\rho(s)} \tag{3}$$

The rms envelope equations were extended to include the influence of dispersion by A. Garren[5], who proposed to use in lieu of (3), the following modified expression (together with the rms envelope equations (1)-(2)):

$$D''+\Big[\ k_x(s)-\frac{K}{2\sigma_x(\sigma_x+\sigma_y)}\ \Big]D(s)=\frac{1}{\rho(s)} \tag*{(3)$'$}$$

Recently, a more accurate analysis has been done[4], where equation (3)′ was incorporated with the generalized rms-equations then given by:

$$\sigma_x''+k_x(s)\sigma_x-\frac{K}{2(\sigma_x+\sigma_y)}=\frac{\varepsilon_{dx}^{\,2}+(\sigma_x\sigma_x'-DD'<\delta^2>)^2}{\sigma_x(\sigma_x^{\,2}-D^2<\delta^2>)}-\frac{(\sigma_x')^2}{\sigma_x}+\frac{<\delta^2>}{\sigma_x}(\frac{D}{\rho}+D'^2) \tag*{(1)$'$}$$

$$\sigma_y''+k_y(s)\sigma_y-\frac{K}{2(\sigma_x+\sigma_y)}-\frac{\varepsilon_y^{\,2}}{\sigma_y^{\,3}}=0 \tag*{(2)$'$}$$

Where $\varepsilon_{dx}^2=(<x^2>-D^2<\delta^2>)(<p_x^2>-D'^2<\delta^2>)-(<xp_x>-DD'<\delta^2>)^2$ is a new invariant ("generalized emittance"), that replaces the regular rms emittance ε_x in the non-dispersive model (1)-(2), and $<\delta^2>^{1/2}=\sigma_\delta$ is the relative rms momentum spread. Preliminary studies have shown that solutions for the system of coupled equations (1)′, (2)′, (3)′ are in fair agreement with 3-D PIC simulations.[4]

A fitting algorithm based on the improved model described by equations (1)′, (2)′ and (3)′ was used to design a dispersion-matched injection system in the presence of space charge. The code allows the possibility of either determining the periodical solution (envelopes and dispersion function) for a given optical structure or finding lattice values which match the specified input beam to specified output values. The code can be used to model any dispersive focusing channel consisting of quadrupole lenses and dipole bending magnets facilitating, for example, the search for an optimal ring injection lattice. The University of Maryland (UMd) E-ring injection was evaluated using this newly developed tool.

3. Determination of Periodical Solutions

The first step in the analysis was the determination of the periodical solutions in the E-ring since these are used as the fitting condition for the injection line.

The single particle dynamics in the E-ring have been studied in the absence of space charge[6]. For that analysis, a lattice working point of $\nu_x = 7.78$ and $\nu_y = 7.80$ was chosen to avoid all resonances up to 4^{th} order. In the analysis discussed below, the magnetic element values used are those derived from the single particle analysis, but in this case the dynamics are found from equations (1)′, (2)′, (3)′. In all examples, the electron beam was assumed to have an energy of 10 keV, a beam current of 100 mA ($K = 1.5 \times 10^{-3}$) and emmittances of $\varepsilon_{x,y} = (12.5/\pi)\ \pi$ mm mrad. The momentum spread was evaluated for three values: $\sigma_\delta = 0$, 5×10^{-3}, and 1.5×10^{-2}.

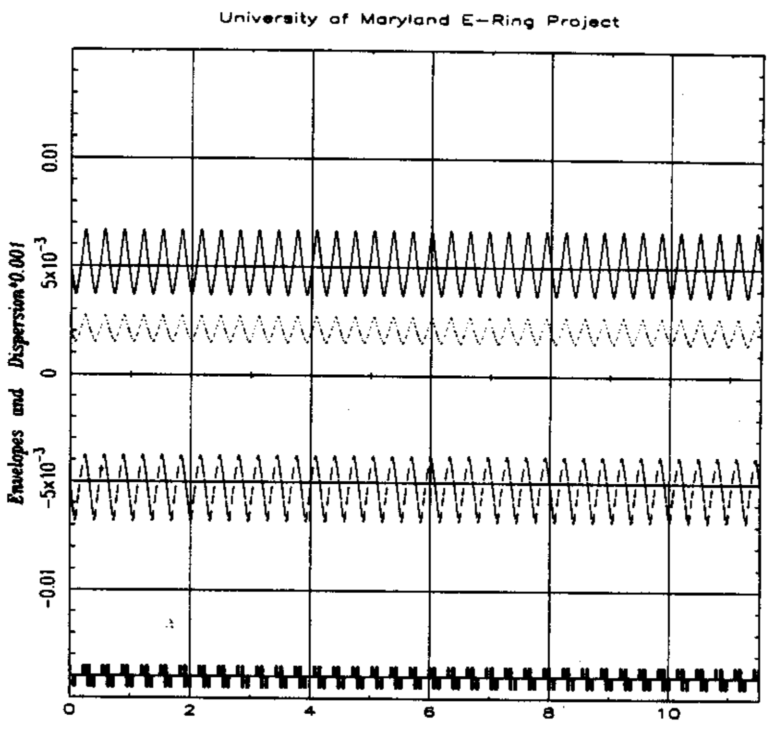

Figure 1. Beam dynamics in the E-ring (36 cells) for a perveance (K) of 1.5×10^{-3} and $\sigma_\delta = 0$. Both envelopes $\sigma_{x,y}$ (solid and dashed lines) and the horizontal dispersion D_x (dotted line) correspond to the ideal periodical solution. Note, that the dispersion is plotted with a multiplying factor 0.001.

Shown in Figure 1 are the periodical envelopes and the dispersion of a high current beam with zero momentum spread. The beam sizes are, of course, much larger than for the zero current case due to the influence of space charge. The values at the injection point are given in Table 1.

Shown in Figure 2 are the periodic solutions for the envelopes and dispersion for the case of $\sigma_\delta = 5 \times 10^{-3}$. The values at the injection point are given in Table 1.

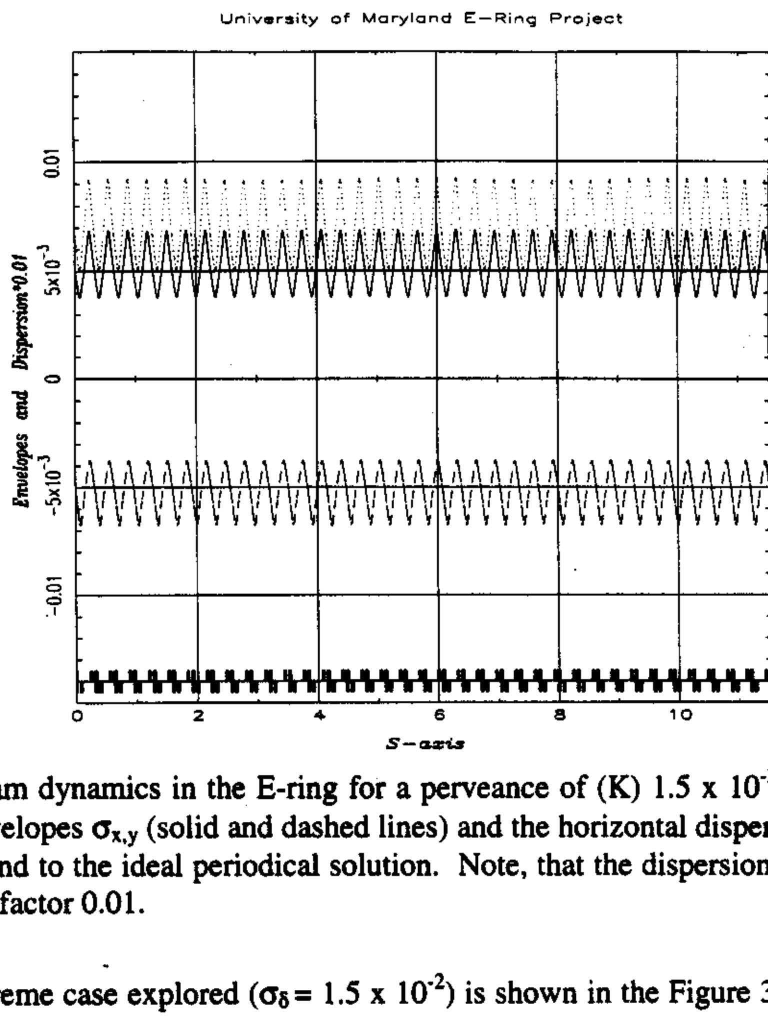

Figure 2. Beam dynamics in the E-ring for a perveance of (K) 1.5×10^{-3} and $\sigma_\delta = 5 \times 10^{-3}$. Both envelopes $\sigma_{x,y}$ (solid and dashed lines) and the horizontal dispersion D_x (dotted line) correspond to the ideal periodical solution. Note, that the dispersion is plotted with a multiplying factor 0.01.

The most extreme case explored ($\sigma_\delta = 1.5 \times 10^{-2}$) is shown in the Figure 3. The values at the injection point are given in Table 1.

σ_δ	σ_x [m]	σ'_x	σ_y [m]	σ'_y	D_x [m]	D'_x
0	5.0×10^{-3}	-2.123×10^{-2}	5.11×10^{-3}	2.16×10^{-2}	2.024	-8.59
5×10^{-3}	5.12×10^{-3}	-2.186×10^{-2}	5.07×10^{-3}	2.14×10^{-2}	0.683	-2.91
1.5×10^{-2}	5.38×10^{-3}	-2.32×10^{-2}	4.98×10^{-3}	2.11×10^{-2}	0.293	-1.262

Table 1. The matched beam parameters (rms envelopes and the dispersion) at the injection point (in the middle of the bending magnet), corresponding to the periodical ring solutions shown in Figure 1 - Figure 3.

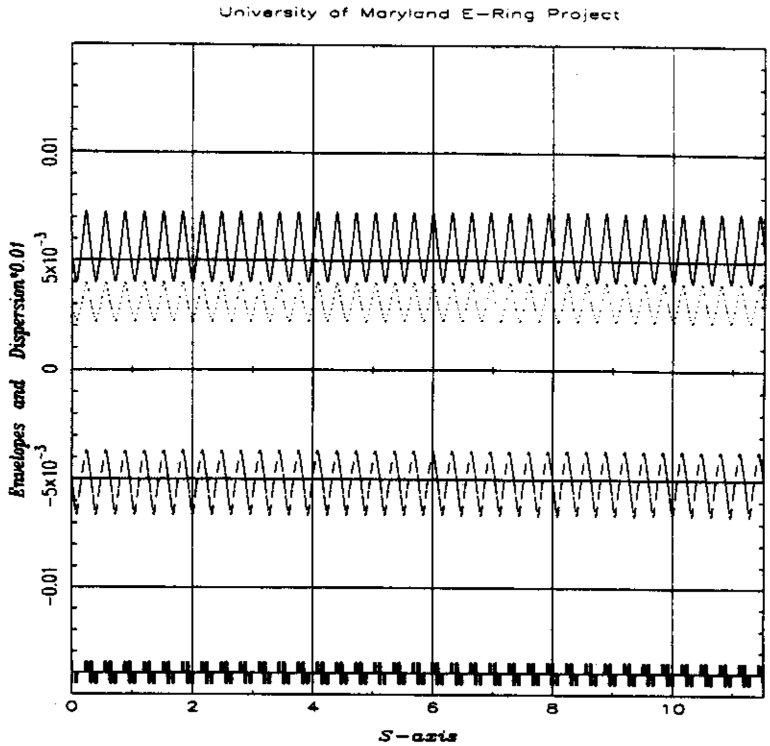

Figure 3. Beam dynamics in the E-ring for a perveance of (K) 1.5×10^{-3} and $\sigma_\delta = 1.5 \times 10^{-2}$. Both envelopes $\sigma_{x,y}$ (solid and dashed lines) and the horizontal dispersion D_x (dotted line) correspond to the ideal periodical solution. Note, that the dispersion is plotted with a multiplying factor 0.01.

4. Injection System Design

For the last case of section 3 ($K = 1.5 \times 10^{-3}$, $\sigma_\delta = 1.5 \times 10^{-2}$), two possible injection systems were evaluated. The geometrical constraints are shown in a layout done from a for a non-dispersive injection system designed earlier.[7] See Figure 4 where the injection point assumed to derive the matching conditions in section 3 is the middle of the dipole labeled D1.

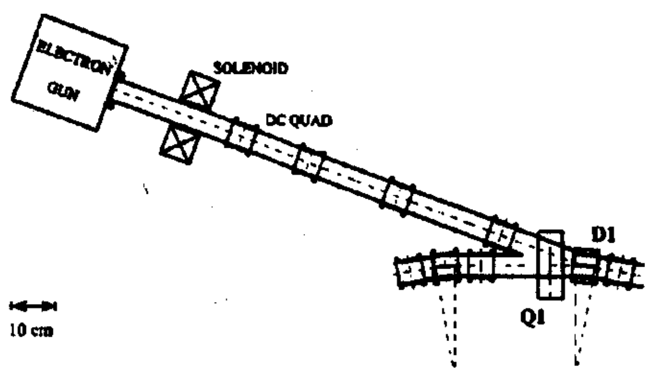

Figure 4. The injection line without dipole magnets, injecting the beam in the E-ring with zero dispersion[7].

An axially symmetrical beam (double crossover) with no dispersion was assumed at the entrance of the injection system. In the cases evaluated, the injection line begins with an initial drift of 15 cm and the minimal distance between all optical elements is ≥ 3 cm. The injected beam matches into the ring lattice at the mid point of a pulsed dipole magnet (D1 in Figure 4), which deflects the beam by the -10° (during injection) and by +10° (after injection). To avoid mechanical interference, the distance from D1 and the last quadrupole lens of the injection line should be ≥18 cm (See the Figure 4.).

Six simultaneous constraints were satisfied during the optimization ($\sigma_{x,y}$ $\sigma'_{x,y}$, and D_x, D'_x) corresponding to the values for the periodical solutions given in Figure 1- Figure 3 and Table 1.

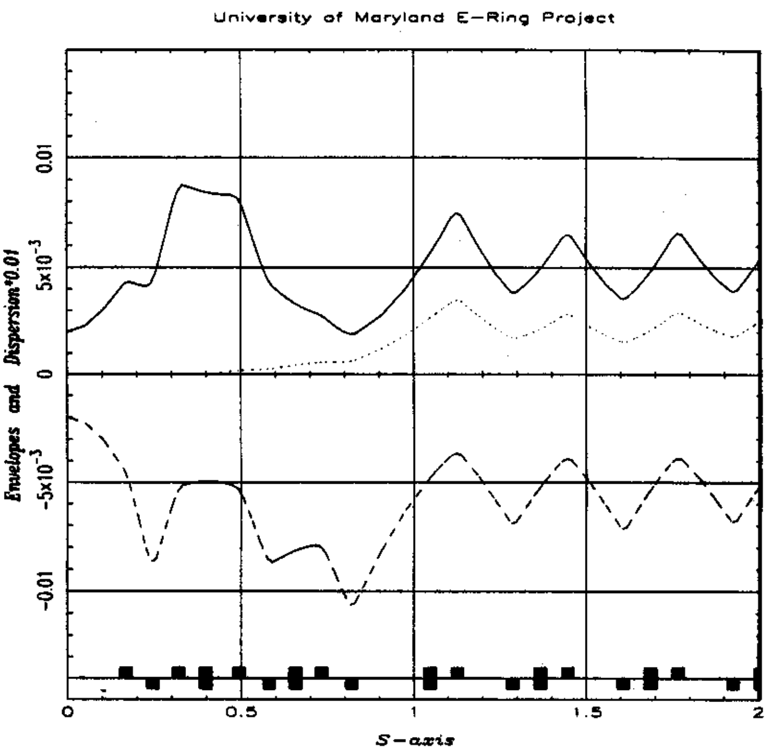

Figure 5. Seven quad injection line solution (variant I of Table 2.)

The solution given for seven quadrupole lenses (See Figure 5.), though requiring additional hardware, has somewhat more favorable envelopes when compared to that with five quadrupoles (See Figure 6.) as would be expected. The lattice data for both variants is given in Table 2. Note that the rms envelopes ($\sigma_{x,y}$) are plotted, and hence the actual beam size will be larger (≅2x). However, the vacuum pipe radius will be ≅2.45 cm, and therefore, this should not be an issue.

N	Length [m] I variant (N_{quads} = 7)	Length [m] II variant (N_{quads} = 5)	$k_x(s)$ [m^{-2}] I variant (N_{quads} = 7)	$k_x(s)$ [m^{-2}] II variant (N_{quads} = 5)	$1/\rho(s)$ [m^{-1}] (bend angle)
1	0.15	0.15	0	0	0
2	0.036	0	215	0	0
3	0.04	0	0	0	0
4	0.036	0.036	-400	-416	0
5	0.04	0.0418	0	0	0
6	0.036	0.036	243	377.9	0
7	0.04	0.034	0	0	0
8	0.0376	0.0376	0	0	4.65 (10^o)
9	0.06	0.0862	0	0	0
10	0.036	0.036	178	-143	0
11	0.05	0	0	0	0
12	0.036	0.036	-183	0	0
13	0.04	0.014	0	0	0
14	0.0376	0.0376	0	0	-4.65 (-10^o)
15	0.04	0.0592	0	0	0
16	0.036	0.036	118	285.7	0
17	0.05	0.03	0	0	0
18	0.036	0.036	-194	-331.7	0
19	0.19	0.18	0	0	0
20*	0.0376	0.0376	0	0	-4.65 (-10^o)
21	0.0432	0.0432	0	0	0
22	0.036	0.036	227.9	227.9	0
23	0.124	0.124	0	0	0
24	0.036	0.036	-226.6	-226.6	0
25	0.0432	0.0432	0	0	0
26	0.0376	0.0376	0	0	4.65 (10^o)

Table 2. Lattice data for injection schemes of Figure 5 and Figure 6.

*Position N=20 is the location of D1 in Figure 4.

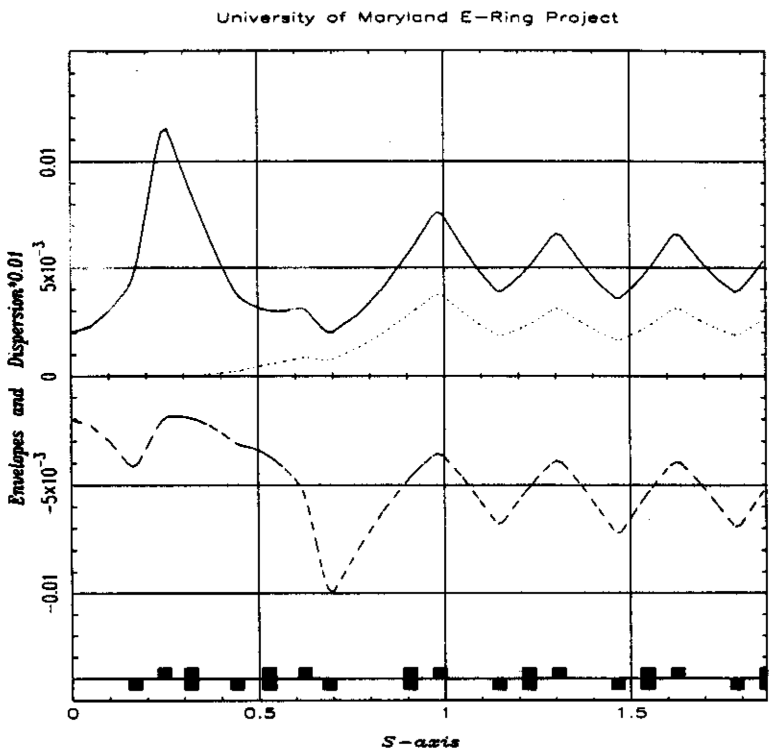

Figure 6. Five quad injection line (variant II of Table 2).

5. Possible Aperiodic Solutions

The ramifications of neglecting dispersion matching were evaluated. The E-ring lattice functions were considered for the condition of zero dispersion at the midpoint of the injection dipole (D1). Three cases ($\sigma_\delta = 0$, 5×10^{-3}, and 1.5×10^{-2}) were evaluated.

Given in Figure 7 is the case for $\sigma_\delta = 0$. Since there is no momentum spread, the beam envelopes are the same as for the case of Figure 1, but the dispersion function is aperiodical.

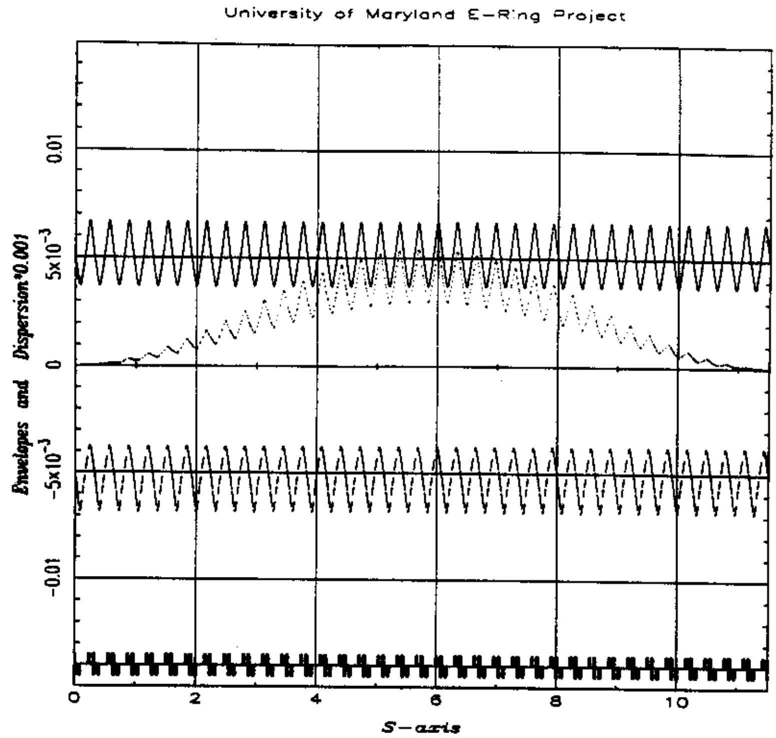

Figure 7. Beam dynamics in the E-ring (36 cells) with perveance (K) 1.5 x 10^{-3} and σ_δ = 0. The initial envelopes are the same as in Table 1 and Figure 1, but the initial dispersion is zero: $D_x(0) = D_x'(0) = 0$.

Given in Figure 8 are the results for σ_δ = 5 x 10^{-3}. With a non-zero momentum spread, the dispersion mismatch perturbs the beam envelopes, and therefore, the beam dynamics become aperiodical.

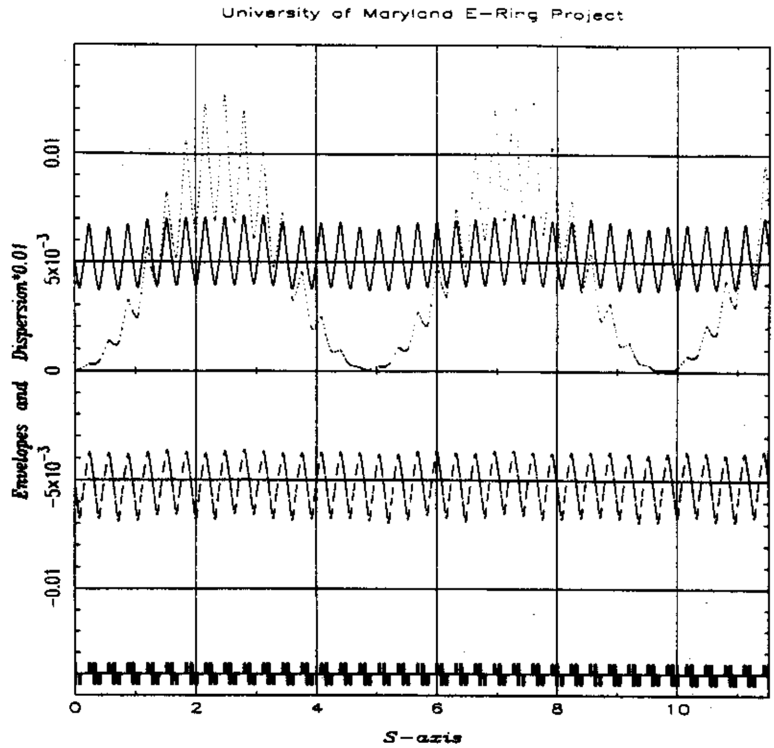

Figure 8. Beam dynamics in the E-ring (36 cells) with perveance (K) 1.5 x 10^{-3} and σ_δ = 5 x 10^{-3}. The initial envelopes are the same as in Table 1 and Figure 2, but the initial dispersion is $D_x(0) = D_x'(0) = 0$.

In the Figure 9, the effect lack of no dispersion matching is most prominent. The resulting envelope perturbation could complicate the E-ring operation since it would effect the beam diagnostic measurements, control, corrections etc.

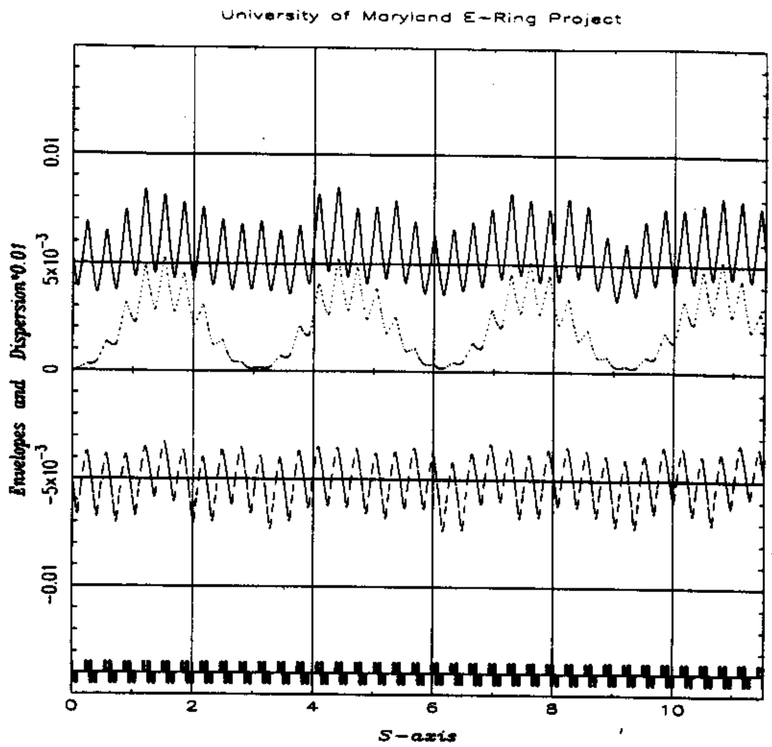

Figure 9. Beam dynamics in the E-ring (36 cells) with the maximum perveance $K = 1.5\times10^{-3}$ and σ_δ = 1.5 x 10^{-2}. The initial envelopes are the same as in Table 1 and Figure 3, but the initial dispersion is $D_x(0) = D_x'(0) = 0$.

6. Discussion.

The recently developed dispersion matching algorithm, based on the generalized set of equations (1)′, (2)′, (3)′ was applied to the UMd E-ring. From this analysis it is concluded that dispersion matching is feasible using standard hardware and will provide better ring performance. Alternative non-dispersion matching schemes are less desirable. However, the validity of the physical model described by equations (1)′, (2)′, and (3)′ should be further verified by comparison with 3D PIC simulations.

Acknowledgements

The authors are grateful to Drs. R.Kishek and M.Venturini (Maryland University) for useful discussions.

References

1. M.Reiser et al. Fusion Eng. Des. **32-33**, 293 (1996). http://www.ipr.umd.edu.ebte/ring/

2. Presentations for the DOE Review of the University of Maryland Electron Ring Project (July 1-2,1997), unpublished.

3. F.J.Sacherer, IEEE Transactions on Nuclear Science NS-18 (1971) 1105.

4. M.Venturini, R.A. Kishek and M.Reiser "Dispersion and Space Charge", Shelter Island Workshop on space charge, AIP Proc. 448, p278 (1998).

5. A. Garren, Proc. Heavy Ion Fusion Workshop, 1979 Report LBL-10301/SLAC-PUB 2575, UC-2, p. 397.

6. L.G. Vorobiev, X. Wu, R.C.York "Single Particle Beam Dynamics Studies for the University of Maryland Electron Ring" MSUCL-1114 (September 1998).

7. T. Godlove, "Injection and Extraction Design", Presentations for the DOE Review of the University of Maryland Electron Ring Project (July 1-2,1997), unpublished.